Prolonged Zero-Order BSA Release from pH-Sensitive Hydrogels of Poly(AAc-*co*-DMAPMA) Having Rich Nano Through Micro Scale Morphology

Anup Das,[1,2] Mohit Mehndiratta,[3] Parthaprasad Chattopadhyay,[3] Alok R. Ray[1,2]

[1]*Centre for Biomedical Engineering, Indian Institute of Technology Delhi, New Delhi 110016, India*
[2]*Biomedical Engineering Unit, All India Institute of Medical Sciences, New Delhi 110029, India*
[3]*Department of Biochemistry, All India Institute of Medical Sciences, New Delhi 110029, India*

Received 24 October 2008; accepted 28 May 2009
DOI 10.1002/app.30968
Published online 1 September 2009 in Wiley InterScience (www.interscience.wiley.com).

ABSTRACT: New variety of pH-sensitive hydrogels, having macroporous interior with honey-comb type architecture and continuous skin at the surface, have been developed by single step aqueous copolymerization of acrylic acid (AAc) and *N*-[3-(dimethylamino)propyl]-methacrylamide (DMAPMA) in different feed ratios at 41 ± 1°C. Interlocked nanogels of ~ 300 nm were identified as the building blocks in all of these cylindrical poly(-AAc-*co*-DMAPMA) matrices (PDMAAc). The gels showed good compressive strength even at a swelling as high as 4330% (mass) at pH 7.0. Morphology of McCoy fibroblast cell line remained unchanged in direct contact with different PDMAAc gels, and cell viability (±SD) was recorded to be in the range of 105 (±3)% to 87 (±8)% after 72 h. Bovine serum albumin (BSA) loaded gels were prepared by means of equilibrium partitioning. Loading efficiency of PDMAAc gels has been found to be in the range of 210–277 mg/g dry gel. BSA release from PDMAAc gels at 37°C has been found to follow non-Fickian diffusion mechanism in simulated gastric juice (pH 1.2), and Case II transport in simulated intestinal juice (pH 7.4). *In vitro* study showed that the gels are capable of retaining >95% of the loaded BSA in gastric medium through average gastric emptying period. Again, ~ 56% BSA release was recorded in 24 h at pH 7.4, indicating prolonged BSA diffusion in intestinal condition. Constant rate of BSA diffusion was reflected from the release profiles at both the pH. Diffusion exponents also supported the same and indicated for absolute zero-order kinetics at pH 7.4. © 2009 Wiley Periodicals, Inc. J Appl Polym Sci 115: 393–403, 2010

Key words: acrylic acid; hydrogels; morphology; pH sensitive; proteins

INTRODUCTION

The advancements in the field like molecular biology and biotechnology not only introduced a large number of new pharmaceutically active peptides and proteins, but also made it feasible to produce them in large quantities with purity and preserved biological activity. This has led the protein-based drugs to become as an important class of treatment agents. Although the oral route is the most convenient and comfortable way of administering drugs, the common strategy for the delivery of protein drugs is frequent injections. For oral protein delivery, colon was found to be the suitable site of absorption.[1,2] A number of oral dosage forms, such as enteric-coated systems and liposomes have been used in commercial applications. These techniques have the potential advantage of high drug-loading. However, a major limitation is that these systems cannot fully protect the drugs and release them at a targeted area with a precisely controllable rate.[3] pH-sensitive hydrogels (PSHs) have been investigated extensively over the past two decades and have attracted significant attention for oral protein delivery. Considerable effort has been made in studying the pH-controlled protein release behavior from various PSHs.[4,5] There are various factors that are needed to be considered to design efficient oral dosage forms, such as drug-loading efficiency, release kinetics, protection from proteolysis, and permeability across GI mucosal epithelia (bioavailability). These, in turn, depend on the concerned hydrogel characteristics like hydrogel type, degree of swelling, swelling kinetics, molecular interaction with proteins, enzyme inhibitory activity, mucoadhesivity, and retention time at various GI compartments.[6–9] Mechanical strength/integrity of the gel during the lifetime of application is equally an important factor. The swollen gel should be strong enough to withstand repeated peristaltic contractions in the GI tract.[7] Apart from all these,

Additional Supporting Information may be found in the online version of this article

Correspondence to: A. R. Ray (alokray@cbme.iitd.ac.in).

cytocompatibility is a must criterion for any material to be used *in vivo*.[10] Reasonably, it is difficult to add all of these functionalities in a single device.

Wide variety of synthetic/natural polymers and their combinations are being constantly investigated to tailor-make the desired hydrogels. However, along with the advantages, each formulation brings with it its own limitation, and thus, creates demand for further optimization. For example, it is the weakly swellable hydrogels that are mostly investigated for controlled delivery of therapeutic drugs. Prolonged drug diffusion from a finite drug source being the major advantage.[4,11] Nevertheless, poor drug-loading efficiency remains as one of the major limitations with most of these hydrogels when the drug is loaded through equilibrium partitioning. Superabsorbent hydrogels, on the other hand, have high loading efficiency (due to high swelling/equilibrium partitioning). However, the drug release rate in most of these gels has been found to be considerably fast due to the rapid and high water uptake.[12]

Added to the suitable loading efficiency and sustained drug release, zero-order release kinetics for prolonged time is a much sought after property for controlled-release devices.[13] A number of sophisticated strategies and tailor-made devices have emerged. For example, hydrogels with nonuniform drug distribution, and rate controlling-barriers on the surface such as higher crosslinked outer edges.[14–16] Even so, designing monolithic hydrogels for providing 12 or 24 h zero-order release kinetics, and eliminating the initial burst release are often difficult and unsuccessful.[17,18] Recently, Wang et al. developed superabsorbent hydrogel based on crosslinked chondroitin sulfate for sustained delivery of therapeutic proteins.[19] The gel was found to release $\sim$ 80% of the loaded protein within 6 h. The release profile, although too fast in comparison with the weakly swellable gels, was reasonably termed as "moderately controlled."

The aim of this work was to develop PSH as oral protein delivery system with many sought after functionalities introduced in a single formulation. In a previous work, we have reported that hydrogel membranes that are stable in simulated body fluid can be prepared without using any chemical crosslinker or radiation. The membranes were prepared simply by aqueous copolymerization of two easily available monomers, viz., acrylic acid (AAc) and *N*-[3-(dimethylamino)propyl]-methacrylamide (DMAPMA), at 41 $\pm$ 1°C.[20] In this work, modified reaction conditions enabled us to fabricate cylindrical gels having continuous skin at the lateral wall, macroporous interior, and interlocked nanogels as the stable building blocks. A series of poly(AAc-*co*-DMAPMA) hydrogels have been prepared, abbreviated as PDMAAc72-PDMAAc90 with the numeric

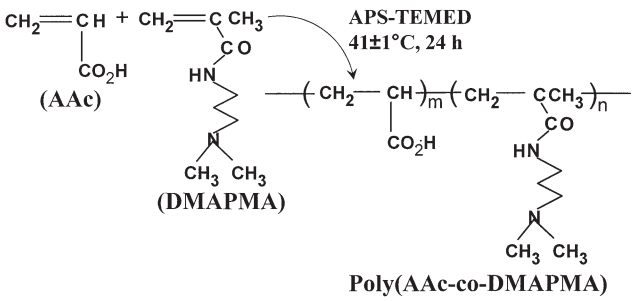

Scheme 1 Synthesis of poly(AAc-*co*-DMAPMA) hydrogel.

representing the AAc content (mol %) in respective gels. Important properties of PDMAAc gels, such as morphology, swelling kinetics, water transport mechanism, mechanical properties, drug loading efficiency, release kinetics, release mechanism, and cytocompatibility were investigated. Relevant experiments were carried out in buffered solutions of various pH ranging from 1 to 10. Bovine serum albumin (BSA), an oval shaped protein having isoelectric point (p*I*) at 4.7 and solubility in water being 40 mg/mL at 25°C,[3] was chosen as the model protein drug. Poly(AAc) and its derivatives like Carbopol have been well documented as having mucoadhesivity and enzyme inhibitory activity.[9,7] PDMAAc gels, having poly(AAc) fraction as the major component, are expected to have enzyme inhibitory activity and may enhance the protein absorption/bioavailability.

EXPERIMENTAL

Materials

Acrylic acid (AAc) of purity 99.5% was purchased from G.S. Chemicals, India. *N*-3-[Dimethylamino)-propyl]-methacrylamide (DMAPMA) of purity 99% was purchased from Aldrich (St. Louis, MO). BSA of molecular weight 66 kDa, purity 96% was purchased from Sigma. Ammonium persulfate (APS) and 2-butanone were purchased from Qualigens Fine Chemicals, India. *N*,*N*,*N*′,*N*′-tetramethyl ethylene diamine (TEMED) was purchased from SRL Pvt. Ltd., India. Chemicals were used without further purification if not otherwise mentioned.

Synthesis of PDMAAc hydrogels

The cylindrical hydrogels of four different monomer feed compositions were prepared by free radical aqueous copolymerization of AAc and DMAPMA, using APS and TEMED as the initiator and accelerator, respectively. The reactions, as shown in Scheme 1, were carried out with slight modification in the technique as described earlier.[20]

Briefly, preformed monomer-water mixtures were kept stirring at $\sim 0^{\circ}C$ in individual round-bottom flasks with a controlled speed to avoid bubble formation. Nitrogen gas was purged into the flasks for 15 min followed by the addition of TEMED (3.0 mol %) and concentrated aqueous solution of APS (amounting 0.50 mol % of monomer) with continuous stirring over magnetic stirrer. After 5 min, the individual reaction mixtures were transferred into cylindrical molds of poly(vinyl chloride) with an internal diameter and length of 3 and 80 mm, respectively. The molds were then placed vertically in a thermostated water bath at $41 \pm 1^{\circ}C$ and dipped up to the height of reaction mixtures. After 24 h of reaction, PDMAAc hydrogels were removed from the molds, cut into pieces, washed in regularly changed distilled water for 3 days to remove the unreacted monomers, and dried in vacuum. According to the molar concentration of AAc in the feed, the gels have been assigned sample code as PDMAAc72, PDMAAc80, PDMAAc86, and PDMAAc90. The feed composition of the four PDMAAc gels is listed in Supporting Information Table SI.

Fourier transform infrared spectroscopy

IR spectra were taken within the range 4000–400 cm^{-1} as KBr pellets on a Nicolet (Madison) Fourier transform infrared (FTIR) spectrophotometer (Model Protege 460). Finely ground powder of freeze-dried samples were used to prepare the KBr pellets.

Scanning electron microscopy

ZEISS EVO series scanning electron microscope (SEM; Model EVO 50) was used to investigate the morphology of PDMAAc gels. All the gels were swollen in PBS of pH 7.4. The swollen samples were snap-frozen by using liquid nitrogen, lyophilized and kept in vacuum till silver sputtering treatment.

Solubility and swelling experiment

Solubility of PDMAAc gels was checked at room temperature as well as on heating in saline water and buffered solution of pH 1–12. Approximately 10 mg polymer was suspended over 20 mL of chosen solvent and the solubility was verified after 2 h.

Degree of swelling was determined by gravimetric method. Dry cylindrical PDMAAc samples of ~ 4 mm in length were swollen in buffered solution of various pH at $37 \pm 1^{\circ}C$. Each sample was removed from the solutions at regular intervals, the surface water was carefully soaked and the weight was recorded till equilibrium swelling. The swelling ratio (Q) was then calculated as $(W_t - W_i)/W_i \times 100$, where W_i is the weight of dry gel and W_t is the weight of the swollen gel at time t.

Mechanical characterization

TA-XT2i Texture Analyzer (Stable Micro Systems, UK) with a 5 kg load cell was used in our experiments. The cylindrical PDMAAc samples were equilibrated in buffered solution pH 7.0. The swollen cylinders were then cut in pieces of ~ 4 mm height by a twin blade chopper. Uniaxial compression experiments were performed on the cut pieces at room temperature with a cylindrical aluminum probe of 35 mm diameter (P35). The pretest speed and the post-test speed were set up at 2.00 mm/s and 1.00 mm/s, respectively, with an acquisition rate of 200 points/s. The force necessary for compressing the hydrogels at 2 mm (test speed 1.00 mm/s) and at break point (test speed 2.00 mm/s) was recorded to determine elastic modulus and compressive strength, respectively. The stress values (σ) were determined using eq. (1).[21]

$$\sigma = \frac{F}{A} \tag{1}$$

where F is the force and A is the cross-sectional area of the strained specimen. All data were obtained in triplicate.

Stress–strain measurements

The parameters generated by the instrument were force and time/displacement. Those information were then converted to elastic modulus, E, by using following equation.

$$\sigma = E(\lambda - \lambda^{-2}) \tag{2}$$

E was determined from the slope of the stress–strain relationship. The macroscopic deformation ratio (λ) was calculated as $\lambda = L_t/L_0$. Here, L_t and L_0 are the length of the deformed and undeformed specimen, respectively.

Compressive strength

To evaluate the compressive strength (stress at break point), the instrument was programmed to deform the samples up to 75%.

Cytotoxicity test

Cytotoxic effects of PDMAAc hydrogels were studied by evaluating cell viability in "Indirect contact" cytotoxicity assay, and general morphological assessment in "Direct contact" test.

Cell culture

McCoy mouse fibroblast cells (ATCC CRL 1696) were used for cytotoxicity test. The cell was routinely cultured and maintained in 25 cm^2 tissue culture flask (Corning) in DMEM medium (Sigma) containing 10% FBS (Sigma), 10 μg/mL ciprofloxacin, and 5% CO_2.

Extract preparation

The cytotoxicity assay of the PDMAAc gels was carried out according to ISO 10993–5 (1992). The cylindrical PDMAAc gels, equilibrated in PBS of pH 7.4, were cut into uniform pieces of 0.2 cm × 0.5 cm (thickness × diameter). Sampling detail is provided in the Supporting Information. The samples were kept in PBS and then sterilized by autoclaving at 120°C for 20 min. One milliliter of culture media was added to two pieces of each kind of PDMAAc samples in a 24-well plate (Corning), and incubated at 37°C for 48 h with 5% CO_2. The extract thus obtained was used for the cytotoxicity test.

"Indirect contact" cytotoxicity assay

Ninety-six–well tissue culture plates (Corning) were prepared by the addition of the hydrogel-extract (50 μL/well in quadruplicate) of each type. The cells were trypsinized and resuspended in culture media. Cell density was determined by hemocytometer. This was followed by the addition of 50 μL/ well of the cell suspension (∼ 3000 cells) in all wells containing gel extract. Blank was prepared with culture medium without cells and a negative control was prepared with culture medium and cells, both in quadruplicates. The plates were then incubated with 5% CO_2.

After 72 h, CellTiter 96® AQueous One Solution Reagent (Promega) was used to assess the cytotoxicity as per manufacturer's protocol. The readings were taken after 4 h at 492 nm using ELISA plate reader (Anthos HT 1).

Morphological assessment—"Direct contact" test

Morphology of McCoy cells in direct contact of PDMAAc gels was studied and compared with that of the cells in negative control. Photographs of the cultured cells were captured randomly after 72 h of incubation.

Statistic analysis

The percentage survival was calculated as [(absorbance of test − absorbance of blank)/(absorbance of control − absorbance of blank)] × 100. Statistical analysis was performed by using *t*-test. A *P*-value of <0.05 was considered significant.

BSA assay

Gel loading

BSA solution of concentration ∼ 20.0 mg/mL was prepared in PBS of pH 7.4. Dry gels of ∼ 6 mm in length were immersed separately in fresh BSA solutions and kept at 4°C. After 24 h, the swollen gels were rinsed carefully with PBS to remove the free BSA from the surface, and dried under vacuum at 25°C. Amount of BSA remained in the respective supernatants was determined by Lowry's method.[22] Briefly, the BSA samples were mixed with a reagent containing solutions of sodium hydroxide, sodium carbonate and copper sulfate in proper ratio. Later, these were treated with Folin's reagent and the absorbance was measured at 750 nm. Loading efficiency of each gel was evaluated from the change of protein content in the solution before and after loading. Each loading experiment was carried out in triplicate. The experimental BSA (Exp. BSA) loading was obtained by using the following equation:

$$\text{Exp.BSA} = \frac{w}{W} \tag{3}$$

where w and W are the mass of BSA loaded (mg) and the mass of dry gel (g), respectively. The predicted protein loading (Pred. BSA) was calculated using the following equation.

$$\text{Pred.BSA} = vC \tag{4}$$

where v and C are respectively the volume (mL) of BSA solution absorbed per gram of dry gel during loading, and the concentration of the BSA loading solution (mg/mL). Equation (4) is based on some assumptions as described elsewhere.[23]

In vitro release

Dry BSA-loaded PDMAAc gels were immersed separately in 25 mL simulated gastric fluid (0.1*N* hydrogen chloride, pH 1.2) and simulated intestinal fluid (phosphate buffer, pH 7.4), and left shaking (100 rpm) in an incubator at 37 ± 1°C. At regular intervals, 1 mL of the samples were withdrawn and replaced by 1 mL of fresh fluid. The amount of BSA in the withdrawn samples was estimated by Lowry's method. The experimental condition should not lead to considerable deviation from an ideal sink condition. It was only 0.05 g of the dry gels (approximately), containing ∼ 0.013 g of BSA, which was suspended in 25 mL of the release media. Furthermore, the release experiments were carried out for

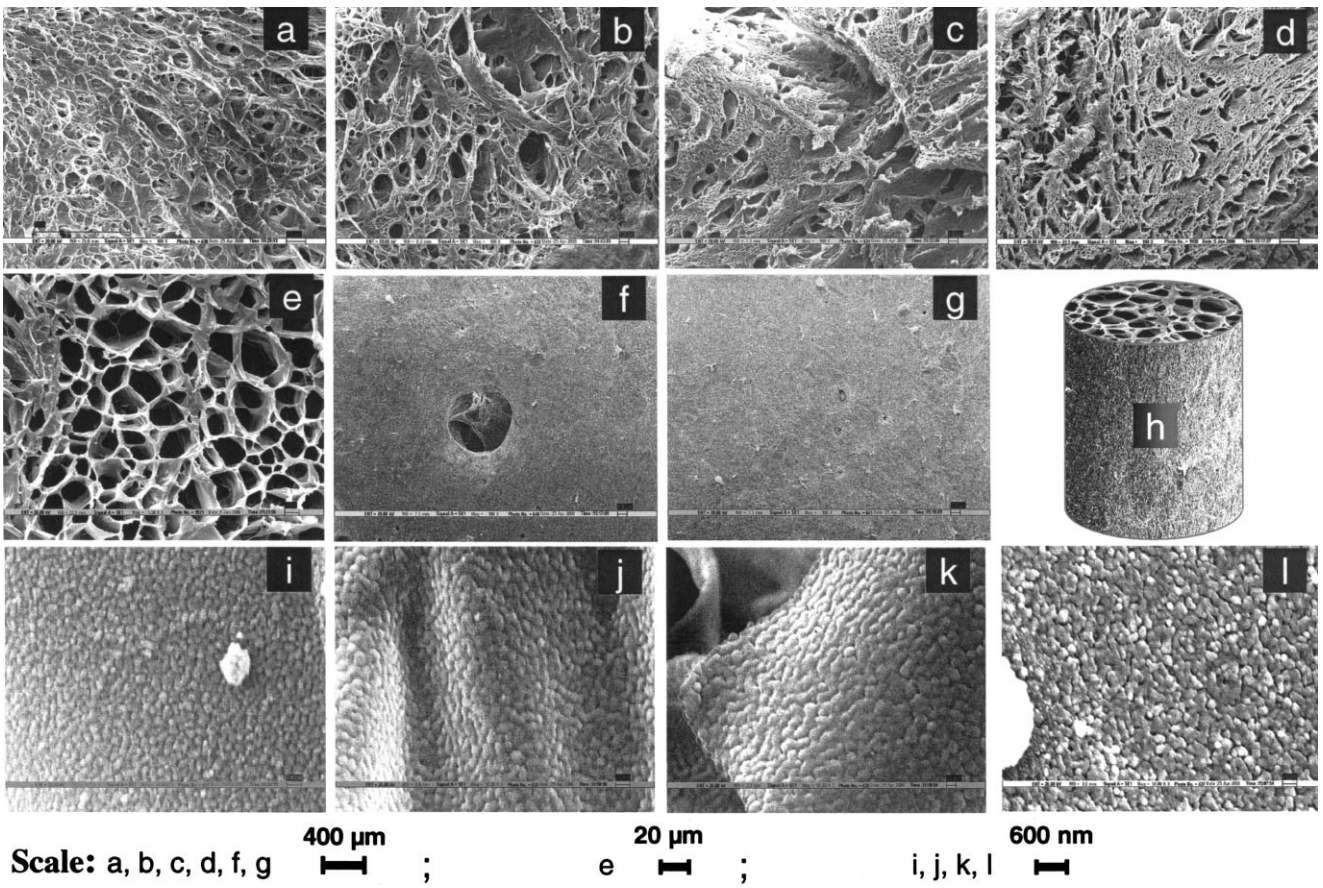

Figure 1 SEM micrographs of cylindrical PDMAAc gels after swelling in PBS of pH 7.4: (a–d) shows the cross-section of PDMAAc72, PDMAAc80, PDMAAc86, and PDMAAc90 respectively at 100× magnification; (e) represents the cross-section of PDMAAc90 at 15 k ×; (f, g) shows the lateral surface of PDMAAc86 and PDMAAc90 respectively at 100×; (h) represents model of PDMAAc90; (i–l) shows the building blocks in PDMAAc72, PDMAAc80, PDMAAc86, and PDMAAc90 respectively at 50 k × magnification.

24 h, which led only to a fractional release of the loaded BSA. Therefore, the small change in the concentration of BSA in the release media over time was expected not to result much disturbance to the sink condition.

RESULTS AND DISCUSSION

FTIR analysis

IR spectra of PDMAAc samples are shown in Supporting Information Figure S1.

Absorption bands at $\sim$ 3432 cm^{-1}, $\sim$ 1666 cm^{-1}, and $\sim$ 1580 cm^{-1} were assigned to N—H stretching, amide I, and amide II respectively of the DMAPMA units. The strong band at $\sim$ 1722 cm^{-1} was due to the stretching vibration of carbonyl group in AAc units. Gradual increase in the intensity of the peak at 1722 cm^{-1} is an evidence of the increase in AAc contents from PDMAAc72 to PDMAAc90. Otherwise, gradual decrease in the peak intensity at 1666 cm^{-1} and 1580 cm^{-1} from PDMAAc72 to PDMAAc90 indicates decrease of DMAPMA content in the same order.

SEM micrographs and morphology

SEM micrographs of the swollen PDMAAc hydrogels are shown in Figure 1.

Figure 1(a–d) represents the cross-sectional view of the gels in the order of PDMAAc72-PDMAAc90. These micrographs indicated that the interior of the gels is macroporous with diameter (or length) ranging around 100–200 μm. However, further magnification revealed that the interior of PDMAAc86 and PDMAAc90 are basically like a honey comb, having uniform porosity of 10–20 μm in diameter. Figure 1(e), the magnified version of Figure 1(d), represents the honey-comb type interior of PDMAAc90. Morphology of the external surface of the lateral wall in cylindrical PDMAAc gels was found to be entirely different. Figure 1(f,g) represents the morphology of the lateral surface in PDMAAc86 and PDMAAc90, respectively. Unlike interior, the surface is not

macroporous, and a continuous skin encompasses it. Few holes, as shown in Figure 1(f), appeared as the defect of the continuous skin. SEM micrographs were captured where the holes were found to be mostly populated. Based on these micrographs, a three-dimensional image of swollen PDMAAc gels is drawn and shown in Figure 1(h).

Another interesting structural feature of PDMAAc gels was revealed when the SEM micrographs were captured at much higher magnification. Figure 1(i–l) shows the micrographs where the cross-sections of PDMAAc72-PDMAAc90 were magnified by 50 k×. All the gels were found to be composed of closely packed nanogels of ~ 300 nm diameter. These micrographs also reveal that the uniformly organized nanogels remain interlocked and do not disintegrate in a medium like PBS which causes swelling as high as 4000% (approximately). This is a rare finding that makes PDMAAc gels unique of its kind. Analysis of the mechanistic aspect of the formation of these nanogels is beyond the scope of this article. It needs comprehensive investigation to delineate the mechanism, which may potentially address the queries like how the monomers/polymers get organized in molecular level to construct these structural units, or what drives these units to arrange uniformly and get interlocked *in situ*, or how the lateral skin develops to encompass the porous interior. The SEM micrographs at least suggest that the interlocked nanogels act as the stable building blocks in PDMAAc gel matrices. It is worth mentioning here that the reproducibility of all PDMAAc gels with characteristic morphology (interlocked nanogels, macroporous interior, and lateral skin) has been ensured by performing the reaction and subsequent characterization several times in the last few years.

Solubility and swelling characteristics

Solubility

All the PDMAAc gels were found to be insoluble in saline water as well as in buffered solution, irrespective of the pH. Even being devoid of any conventional crosslinker, all the gels remained dimensionally stable. This is quite an interesting and unexpected result. A copolymer predominantly consisting of AAc is not expected to remain stable and insoluble in alkaline condition. It inspired us to investigate whether any impurity possibly present in the monomers play any role in the exceptional dimensional stability of the PDMAAc gels. Similar gels were prepared with the two monomers purified by vacuum distillation. Interestingly, the gels still remain insoluble. Again, stability due to thermal crosslinking is unlikely because of the following reasons: (1) PDMAAc copolymers were prepared at 41 ± 1°C in thermostat, (2) dilute monomer mixtures were used to avoid auto acceleration during polymerization reaction, and (3) the reactions took ~ 24 h to fabricate the solid PDMAAc products, which ensure slow polymerization and, thus, rule out the possibility of heat accumulation. Therefore, as mentioned earlier, a comprehensive investigation is needed to find the nature of crosslinking and elucidate the unusual stability of PDMAAc gels.

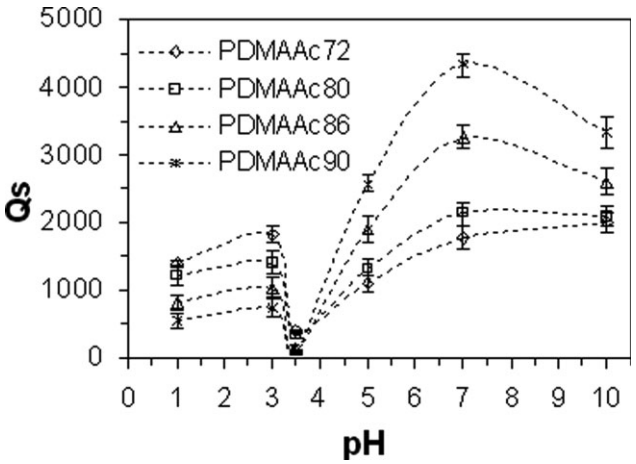

Figure 2 Equilibrium swelling (Q_s) of different PDMAAc gels in buffered solution of various pH at 37 ± 1°C (N = 3, ±SD).

Effect of copolymer composition on pH-dependent swelling behavior

Equilibrium swelling of PDMAAc hydrogel, its variation with monomer composition and pH of the medium are shown in Figure 2.

Swelling behavior of a typical polyampholyte, with an isoelectric point (pI) at ~ 3.5, was observed. Swelling of PDMAAc hydrogels at pH < pI is mainly due to the ionization (protonation) of the DMAPMA units [$-N(CH_3)_2H^+$]. Whereas, ionization (deprotonation) of the AAc units ($-COO^-$, $pK_a \approx$ 4.5) at pH > pI accounts for the swelling at higher pH. Reasonably, increasing DMAPMA content increases the swelling ratio of PDMAAc gels at lower pH, and increasing AAc content does the same at higher pH.

Swelling profile of individual PDMAAc gels against time at pH 1.0 and 7.0 are shown in Supporting Information Figures S2 and S3, respectively. Although the PDMAAc gels showed increasing swelling at pH > 3.5, the ampholytic nature may drive the gels to be more colon-specific as drug carrier. For details, refer the Supporting Information.

Diffusion

Diffusion of water into a hydrogel may govern the release kinetics of entrapped drug from the matrix.[24]

TABLE I
Diffusion Exponents (n) and Diffusion Constants (K) of PDMAAc Gels During Swelling at pH 1.0 and 7.0

	Diffusion parameters					
	pH 1.0			pH 7.0		
Sample ID	$K \times 10^3$	n	R^2	$K \times 10^3$	n	R^2
PDMAAc72	13.62	0.83	0.99	22.29	0.57	0.99
PDMAAc80	14.06	0.83	0.99	9.47	0.73	0.98
PDMAAc86	28.41	0.65	0.99	4.09	0.87	0.99
PDMAAc90	35.51	0.60	0.99	2.48	0.98	0.99

Diffusion of water into the glassy polymeric matrix generally exhibits a behavior ranging from Fickian to Case II extremes depending on the experimental conditions and thermodynamic compatibility between water and hydrogel.[25] It is known that the initial phase of volume variation in highly swellable gels generally follows zero-order swelling kinetics.[26] Therefore attempts have been made to derive the mechanism of volume variation, at the initial phase, applying the following empirical eq. (5).[27]

$$F = M_t/M_\infty = Kt^n \quad (5)$$

where F represents the fractional water uptake, M_t is the absorbed water at time t, M_∞ is the absorbed water at equilibrium, K is a constant incorporating characteristic of the macromolecular network system, and n is an exponent characteristic to the diffusion mode. Equation (5) is applicable for $F \leq 0.6$, and a plot of ln(F) against ln(t) yields a straight line. For $n = 0.5$; water diffusion follows the well-known Fickian mechanism. Here, water diffusion is mainly controlled by chemical potential gradient and allows no or little volume variation during diffusion. For $n = 1$, Case II diffusion mechanism is followed. The volume variation is proportional to time. The faster stress relaxation rate predominates here, and governs the kinetics of volume variation. The intermediate case, known as anomalous or non-Fickian diffusion, occurs when $0.5 < n < 1.0$.

Ln(F)-ln(t) relationship during water diffusion into PDMAAc hydrogels at pH 1.0 and 7.0 are shown in Figure S4 and S5, respectively. Diffusion exponents (n) and diffusion constants (K) were calculated from the slopes and intercepts of the curves, and are listed in Table I.

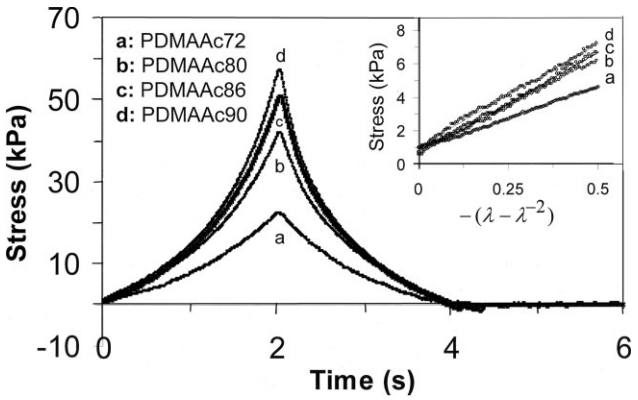

Figure 3 Typical stress-displacement curves of different PDMAAc gels equilibrated in buffer of pH 7.0. Maximum deformation with each sample being 2 mm. Inset: Respective stress–strain curves.

The results indicate that the diffusion mechanism was predominantly non-Fickian in all the gels at either pH.

Mechanical properties

Two kinds of compression experiments, each in triplicate, were carried out. The first kind determines the system hardness (F_{max}) and compressive elastic modulus (E). The second kind was carried out to evaluate the maximum stress that the gels could withstand before breaking (compressive strength, S). Profiles obtained from a typical experiment of the first kind for four PDMAAc gels are shown in Figure 3.

Typical stress-time curves obtained from the second kind of experiment are shown in Figure S6. Results of all the experiments are summarized in Table II.

Figure 3 demonstrates the instantaneous response of the gels toward stress relaxation, amounting equal and opposite to the applied stress. In other words, all the PDMAAc samples behave like typical viscoelastic materials. Linear stress–strain relationship was observed at low strain in all the samples, and is

TABLE II
Variation of Swelling, Hardness, Modulus, and Compressive Strength (S) in PDMAAc Gels at pH 7.0

		System hardness	Elastic modulus		
Sample code	% Swelling (mass)	F_{max} (kPa)	E (kPa)	R^2	S (kPa)
PDMAAc72	1785 ± 162	22.38 ± 0.19	7.39	0.99	164 ± 6.5
PDMAAc80	2130 ± 175	41.96 ± 0.16	10.90	0.99	262 ± 3.9
PDMAAc86	3265 ± 171	52.35 ± 0.22	12.06	0.99	305 ± 8.6
PDMAAc90	4330 ± 179	56.91 ± 0.29	12.21	0.99	322 ± 7.7

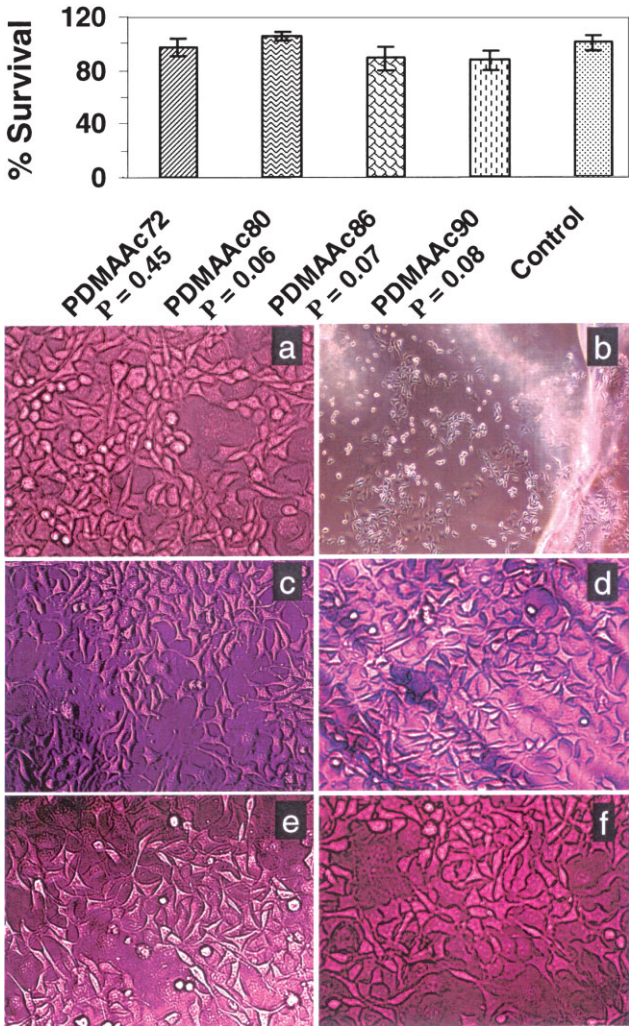

Figure 4 Results of cytotoxicity tests. The bar graph represents cell viability of McCoy cell line after 72 h of incubation with the extracts of different PDMAAc gels and the negative control. *P*-values of the statistical analysis are given next to each sample ID. Optic micrographs represent the randomly captured photographs of McCoy cells with different gels after 72 h. (a) Negative control, captured at ×40 magnification; (b) PDMAAc72, at 10×; (c–f) PDMAAc72, PDMAAc80, PDMAAc86, and PDMAAc90 respectively, at 40×. [Color figure can be viewed in the online issue, which is available at www.interscience.wiley.com.]

shown as inset, Figure 3. Corresponding elastic moduli (*E*), as given in Table II, indicate that the flexibility decreases, or, rigidity increases, from PDMAAc72 to PDMAAc90. Figure 3 also reveals that the hardness increases gradually from PDMAAc72 to PDMAAc90.

The PDMAAc gels were found to remain unbroken at 50% deformation, and fractured somewhere nearer to 75% deformation. However, none of these were completely fragmented at 75% deformation. This may be due to the presence of lateral skin in cylindrical PDMAAc slabs, which acts as protective shell. Hence, the slabs preserve mechanical strength even after partial fracture as evident from Figure S6. Therefore, the values assigned against "*S*" are not absolute but slightly higher than the original, and should more precisely be termed as fracture point instead of break point. All the viscoelastic parameters, viz., hardness, modulus and strength, increase with the AAc content in PDMAAc gels. For details, refer the Supporting Information.

Cytotoxicity study

The results of cytotoxicity assay of PDMAAc gels with XTT technique, and morphological assessment in "Direct contact" test are shown in Figure 4.

The bar-graph in Figure 4 indicates that there is no significant decrease in the viability of McCoy cell line after 72 h of incubation with the extract of PDMAAc gels, when compared with the negative control. The individual viability (±SD) were found to be 96.94 (±6.73)%, 105.13 (±3.42)%, 88.56 (±8.38)%, and 87.01 (±7.71)% for PDMAAc72, PDMAAc80, PDMAAc86, and PDMAAc90, respectively. Corresponding *P*-values, as given next to each sample ID in the bar graph, were found to vary in the range of 0.06–0.45.

Figure 4(a) represents the optic micrograph of McCoy cell line in the control after 72 h. The micrograph in Figure 4(b), captured at 10× magnification, shows the McCoy cells with swollen PDMAAc72. Figure 4(c–f), captured at 40× magnification, show the cells with PDMAAc72-PDMAAc90 respectively. These micrographs ensure the profuse proliferation of McCoy cells in direct contact of PDMAAc gels. It is also evident that the characteristic spindle shaped morphology remains intact. From these results, it can be inferred that the PDMAAc gels have very low cytotoxicity and, as such, show great potential for use in applications like oral drug delivery.

BSA assay

BSA loading

BSA loading efficiency of each of the PDMAAc gels was determined experimentally in triplicate, and the results are reported as the mean ± SD. Predicted and experimental BSA loadings are summarized in Table III.

Experimental BSA of PDMAAc gels was found to be in the range of 210 (±26) to 277 (±24) mg/g dry gel. High loading efficiency was due to the high swelling of the gels in BSA loading solution. Theoretically, the loading efficiency should increase from PDMAAc72 to PDMAAc90 due to the increase in swelling. Experimentally, it was observed that the loading efficiency increases from 210 mg/g in

TABLE III
Comparison of Experimental BSA Loading Efficiency of Different PDMAAc Gels to the Theoretical Values as Predicted from the Respective Degree of Swelling in BSA Solution

Sample code	% Swelling[a] (mass)	BSA loaded (mg/g dry gel)		
		Predicted	Experimental	Difference
PDMAAc72	1523 ± 79	330.85	248.36 ± 13.01	82.49
PDMAAc80	1591 ± 116	334.47	210.89 ± 26.58	123.58
PDMAAc86	2027 ± 172	445.18	246.33 ± 11.01	198.85
PDMAAc90	2338 ± 127	494.48	277.04 ± 24.96	217.44

[a] Swelling of individual PDMAAc gels after 24 h in 2% (w/v) BSA solution in PBS.

PDMAAc80 to 303 mg/g in PDMAAc90. However, in contrary to the predicted trend, the loading efficiency of PDMAAc72 was found to be 248.36 mg/g, which was slightly higher than that of PDMAAc80. This is because of the fact that swelling of PDMAAc72 and PDMAAc80 in BSA solution, as shown in Table III, differs slightly. However, there is a considerable difference in the DMAPMA content in the two gels. The amide groups (—CO—NH—) of the DMAPMA units are expected to induce affinity for the BSA molecules through hydrogen bonding. The enhanced BSA-affinity of PDMAAc72 due to more DMAPMA content most probably predominates over the slightly higher swelling ratio of PDMAAc80. This might have caused off-the-trend increase of BSA loading efficiency in PDMAAc72. Again, the experimental loading efficiency of all the gels were found to be less than the corresponding theoretically predicted values. This is due to the fact that both BSA molecules and the PDMAAc matrices are expected to be negatively charged at pH 7.4 and, hence, impart Coulombic repulsion to each other. The negative charge density is expected to increase from PDMAAc72 to PDMAAc90, and justifies the gradual increase in the difference between predicted and experimental loading efficiencies through PDMAAc72-PDMAAc90.

In vitro BSA release

The release profiles of BSA from PDMAAc90 at pH 1.2 and 7.4 are represented in Figure 5.

Similar profiles, as obtained from PDMAAc86 are shown in Figure S7.

The primary *y*-axis represents the amount of BSA release (mg) per gram of the dry gels. These amounts were then converted into the corresponding values representing percent BSA release per gram of the dry gels, and are shown in the secondary *y*-axis. For convenience, the results are listed in Supporting Information Table SII. Figure 5 indicates steady BSA release rate, or, in other words, zero-order release kinetics from PDMAAc90 in either pH. It is worthwhile to remember here that the PDMAAc hydrogels showed swelling behavior like typical superabsorbents. In contrary, the BSA release rate was found to be considerably slow. It was only 56.08 ± 4.6% and 50.99 ± 3.9% of the loaded BSA per gram of dry PDMAAc86 and PDMAAc90 gels that was recorded to be released in 24 h at pH 7.4. In case of pH 1.2, the amounts were only 20.97 ± 2.4% and 18.16 ± 2.9%, respectively.

Attempts were made to delineate the BSA diffusion mechanism by applying Ritger–Peppas equation for swellable hydrogels (6).[24]

$$F = M_t/M_\infty = kt^n \quad (6)$$

Here, F is the fractional BSA diffusion at time t, M_t represents the amount of BSA released per gram of dry PDMAAc at time t, M_∞ represents the amount of BSA released at infinite time, which is considered to be equivalent to the amount of BSA loaded per gram of dry PDMAAc, n is the diffusional exponent that may determine the diffusion mechanism. Applicability of the aforementioned equation and its limitations in dealing with a system

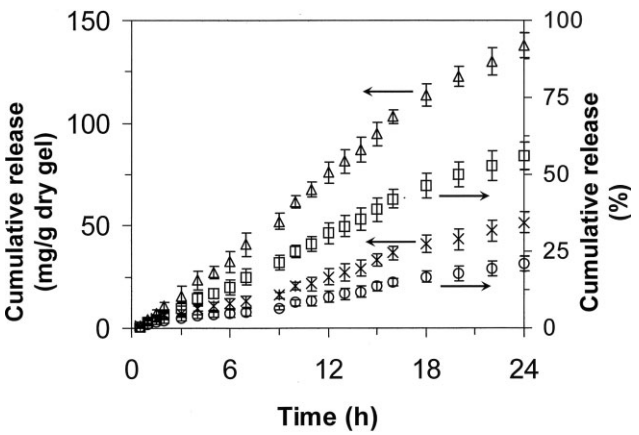

Figure 5 Cumulative release of BSA from PDMAAc90 at 37 ± 1°C in simulated gastric juice (✱, ○) and simulated intestinal juice (△, □). The primary *y*-axis represents the amount (mg) of BSA release per gram of the dry gels. The secondary *y*-axis represents percent BSA release per gram of the dry gels ($N = 3$, ±SD).

TABLE IV
Results of Mathematical Analysis of BSA Diffusion Kinetics

	Diffusion parameters					
	pH 1.2			pH 7.4		
Sample code	$K \times 10^4$	n	R^2	$K \times 10^4$	n	R^2
PDMAAc86	4.86	0.79	0.98	4.67	0.96	0.98
PDMAAc90	4.70	0.81	0.99	4.69	0.97	0.99

like PDMAAc gel is explained in the Supporting Information. Fractional BSA diffusions against time are shown in Figures S8 and S9. Important results are listed in Table IV.

The results indicate that the BSA diffusion at the early stage follows non-Fickian mechanism at pH 1.2, and Case II transport at pH 7.4. The values of n reveal that swelling/chain relaxation plays a major role in the diffusion of BSA at both the pH, and ensures absolute zero-order diffusion kinetics at pH 7.4. The swelling controlled diffusion mechanism cannot explain the slow diffusivity of BSA at pH 1.2 as well as pH 7.4.

In search of plausible explanation, we have tried to compare the rate and mode of BSA diffusion with those of water transport in PDMAAc gels. Exact numerical analysis of diffusional data is not possible with PDMAAc gels. Major limiting factors include high swelling and unusual morphology of PDMAAc gels. In this regard, a comprehensive discussion is included in the Supporting Information. Nevertheless, a comparative kinetic study of water transport and BSA diffusion is possible with the negotiation of precision in individual estimations. The short time approximation of the fractional release is applied to evaluate the diffusion coefficient. Purposefully, relevant semi-empirical eq. (7) was simplified into eq. (8).

$$F = k_1\sqrt{t} + k_2 t = 4\left(\frac{Dt}{\pi l^2}\right)^{\frac{1}{2}} + \frac{2k_0}{C_0 l}t \tag{7}$$

$$F = 4\left(\frac{Dt}{\pi l^2}\right)^{\frac{1}{2}} \tag{8}$$

where F being the fractional diffusion at time t. k_1 correlates the diffusion coefficient (D) due to Fickian transport, k_2 correlates the relaxation constant (k_0) due to Case II transport, and l is the length of the PDMAAc cylinders. Equation (8) is applied to evaluate D for PDMAAc86 and PDMAAc90 at low pH only, where F is controlled simultaneously by diffusion and relaxation. Otherwise, relaxation is the sole operating mechanism at high pH. The plot of F against $t^{0.5}$ at the early stage of swelling and BSA diffusion are given in Figures S10 and S11. The results are listed in Supporting Information Table SIII. Diffusion coefficient [D (cm^2/min)] of BSA at pH 1.2 was found to be 9.04×10^{-7} and 8.24×10^{-7} in PDMAAc86 and PDMAAc90, respectively; Whereas D of water at pH 1 was 2.73×10^{-4} and 2.68×10^{-4}, respectively. Molecular weight of the passenger always play important role in deciding the rate of mass transport. However, available literature indicates, it is unlikely that the huge difference in the D values of water and BSA is solely driven by the difference in molecular weight. Gayet and Fortier calculated the diffusion coefficient of drugs, having different molecular weight, in BSA-PEG hydrogel.[28] The value of D was found to decrease gradually from 15.3×10^{-7} cm^2/s in theophylline to 1.3×10^{-7} cm^2/s in lysozyme. The increase in molecular weight from 180.17 D to 14.4 kD resulted in the decrease of D by a factor of 11.76 only. Again, Coulombic repulsion is expected between BSA and PDMAAc gels due to net positive charge at pH 1.2. The exceptionally slow diffusion of BSA and relatively fast diffusion of water may partially be due to the difference in the respective path of transport. Small water molecules are expected to diffuse along all directions of the gels. In contrary, large BSA molecules are most probably restricted to diffuse only along the axis due to the lateral skin, which appears to be impermeable to BSA. It would be difficult to prove the axial diffusion of BSA by a simple analytical technique. However, a comparative analysis of the BSA diffusion profile in PDMAAc to that in similar hydrogels may lead to a plausible conclusion. Wu et al. studied the BSA diffusion from crosslinked poly(NIPAAm) slabs having dimensions of 10 mm $\times$ 10 mm $\times$ 4 mm (length $\times$ width $\times$ height).[29] One of the PNIPAAm samples, abbreviated as NG3, was found to yield equilibrium swelling ratio ($\sim$ 4000% at 22°C) similar to that of PDMAAc90 (4330% at pH 7.0). The total surface area (360 mm^2), length (10 mm), and thickness (4 mm) in NG3 are higher than those of PDMAAc90 (70.68 mm^2, 6 mm, and 3 mm, respectively). Again, PNIPAAm gels were reported to have strong affinity for BSA molecules. Therefore, rate of BSA diffusion from NG3 at 22°C is expected to be much slower than that of PDMAAc90 at pH 7.4. For an effective comparison of BSA diffusion, it is needed to have similar BSA/dry gel ratio in the concerned gels. Incidentally, the BSA loading efficiency of PDMAAc90 was found to be similar to NG3 when the latter was equilibrated in 1% BSA solution. Therefore, the release profile of these two gels was compared. It was observed that NG3 releases 60% of the loaded BSA in 8 h at 22°C, whereas PDMAAc90 needs >24 h to accomplish 60% release. These data again demonstrate that BSA diffusion in PDMAAc gels is considerably restricted in spite of the fact that BSA molecules experience

strong Coulombic repulsion in PDMAAc gels at pH 7.4. Based on the results of diffusion study and surface morphology, it is believed that the diffusion of BSA in PDMAAc gels is predominantly one dimensional and axial.

CONCLUSIONS

Novel oral protein delivery system PDMAAc has been fabricated to add many sought after functionalities in a single formulation. An easy and convenient method like single-step aqueous copolymerization reaction at near-ambient temperature is worthwhile to mention as it enabled fabrication of otherwise a reasonably sophisticated and tailor-made cylindrical matrix like PDMAAc, where the macroporous interior is covered by continuous lateral wall. Formation of interlocked nanogels *in situ* during the fabrication of these monolithic matrices is a rare finding, which may prove to be the introduction of a novel concept in developing dimensionally stable gels without using conventional crosslinking agents. All the swollen gels remained rigid and were found to have appreciable compressive strength. High swelling ratio, like typical superabsorbents, and macroporous interior enabled the gels to house appreciable amount of BSA. However, rapid BSA release, as was expected from the non-Fickian/Case II water transport mechanism, was overruled by the tailor-made surface morphology. Lateral skin hindered the radial diffusion of giant BSA molecules but one-dimensional axial diffusion through honey-comb type channels along the cross-section, which led to a unique combination of zero-order kinetics and prolonged diffusion time without significant initial burst release. Release experiments in simulated gastric juice for a period of 24 h, which is much longer than average gastric emptying time, suggested that PDMAAc86 and PDMAAc90 are capable of keeping $>95\%$ of the loaded BSA molecules arrested during the passage across stomach. The zero-order kinetics in simulated intestinal juice may prove the gels to be excellent carrier for steady-state therapeutic dose of proteins in the colon. The concept of axial diffusion might have left considerable scope of modulation in the rate of BSA diffusion by simply changing the aspect ratio in PDMAAc gels. PDMAAc gels are expected to have enzyme inhibitory and mucoadhesive properties as poly(AAc) being the major constituent in all the formulations. These two features are currently under verification in our laboratory.

References

1. Akala, E. O.; Kopečková, P.; Kopeček, J. Biomaterials 1998, 19, 1037.
2. Lamprecht, A.; Yamamoto, H.; Takeuchi, H.; Kawashima, Y. J Controlled Release 2004, 98, 1.
3. He, H.; Cao, X.; Lee, L. J. J Controlled Release 2004, 95, 391.
4. Kim, B.; Flamme, K. L.; Peppas, N. A. J Appl Polym Sci 2003, 89, 1606.
5. George, M.; Abraham, T. E. Int J Pharm 2007, 335, 123.
6. Sajeesh, S.; Sharma, C. P. J Appl Polym Sci 2006, 99, 506.
7. Peppasa, N. A.; Buresa, P.; Leobandunga, W.; Ichikawab, H. Eur J Pharm Biopharm 2000, 50, 27.
8. Wu, J. Y.; Liu, S. Q.; Heng, P. W. S.; Yang, Y. Y. J Controlled Release 2005, 102, 361.
9. Kompella, U. B.; Lee, V .H. L. Adv Drug Delivery Rev 2001, 46, 211.
10. Fischer, D.; Li, Y.; Ahlemeyer, B.; Krieglstein, J.; Kissel, T. Biomaterials 2003, 24, 1121.
11. Zhang, X.-Z.; Wu, D.-Q.; Chu, C.-C. Biomaterials 2004, 25, 3793.
12. Lin, Y.-H.; Liang, H.-F.; Chung, C.-K.; Chen, M.-C.; Sung, H.-W. Biomaterials 2005, 26, 2105.
13. Kikkinides, E. S.; Charalambopoulou, G. Ch.; Stubos, A. K.; Kanellopoulos, N. K.; Varelas, C. G.; Steiner, C. A. J Controlled Release 1998, 51, 313.
14. Lee, P. I. J Pharm Sci 1984, 73, 1344.
15. Lu, S.; Anseth, K. S. J Controlled Release 1999, 57, 291.
16. Lee, E. S.; Kim, S. W.; Cardinal, J. R.; Jacobs, H. J Membr Sci 1980, 7, 293.
17. Pillay, V.; Fassihi, R. J Controlled Release 2000, 67, 67.
18. Wu, L.; Brazel, C. S. Int J Pharm 2008, 349, 1.
19. Wang, S.-C.; Chen, B.-H.; Wang, L.-F.; Chen, J.-S. Int J Pharm 2007, 329, 103.
20. Das, A.; Ray, A. R. J Appl Polym Sci 2008, 108, 1273.
21. Muniz, E. C.; Geuskens, G. Macromolecules 2001, 34, 4480.
22. Lowry, O. H.; Rosebrough, N. J.; Farr, A. L.; Randall, R. J. J Biol Chem 1951, 193, 265.
23. Dong, L. C.; Hoffman, A. S. J Controlled Release 1991, 15, 141.
24. Ritger, P. L.; Peppas, N. A. J Controlled Release 1987, 5, 37.
25. Lee, P. I. J Controlled Release 1985, 2, 277.
26. Hamshary, H. E. Eur Polym J 2007, 43, 4830.
27. Said, A. E.-H. A. Biomaterials 2005, 26, 2733.
28. Gayet, J.-C.; Fortier, G. J Controlled Release 1996, 38, 177.
29. Wu, J. Y.; Liu, S. Q., Heng, P. W. S., Yang, Y. Y. J Controlled Release 2005, 102, 361.